
Stratified Learning: a general-purpose statistical method for improved learning under Covariate Shift

Maximilian Autenrieth
Imperial College London
m.autenrieth19@imperial.ac.uk

David van Dyk
Imperial College London
d.van-dyk@imperial.ac.uk

Roberto Trotta
Imperial College London
& SISSA (Trieste)
rtrotta@sissa.it

David Stenning
Simon Fraser University
dstennin@sfu.ca

Abstract

Covariate shift arises when the labelled training (source) data is not representative of the unlabelled (target) data due to systematic differences in the covariate distributions. A supervised model trained on the source data subject to covariate shift may suffer from poor generalization on the target data. We propose a novel, statistically principled and theoretically justified method to improve learning under covariate shift conditions, based on propensity score stratification, a well-established methodology in causal inference. We show that the effects of covariate shift can be reduced or altogether eliminated by conditioning on propensity scores. In practice, this is achieved by fitting learners on subgroups ("strata") constructed by partitioning the data based on the estimated propensity scores, leading to balanced covariates and much-improved target prediction. We demonstrate the effectiveness of our general-purpose method on contemporary research questions in observational cosmology, and on additional benchmark examples, matching or outperforming state-of-the-art importance weighting methods, widely studied in the covariate shift literature. We obtain the best reported AUC (0.958) on the updated "Supernovae photometric classification challenge" and improve upon existing conditional density estimation of galaxy redshift from Sloan Data Sky Survey (SDSS) data.

1 Introduction

In supervised learning, models are trained on labeled objects, with the aim of generalizing the learned pattern by predicting the output of new, unlabeled objects. When the labeled training (source) data is not an accurate representation of the unlabeled (target) data distribution, the learning models may not generalize well to the target data, leading to unreliable target output predictions. The purpose of domain adaptation methods is to obtain accurate target predictions in such situations [60; 64; 7; 47]. Domain adaptation problems are widespread, arising in applications such as in medical imaging [79; 89; 41]; natural language processing [39]; robotics and computer vision [62; 33; 85; 23]; and astronomy, where brighter astronomical objects are more likely to be observed and therefore included in the training set [28; 90; 66]. With increasing interest in the learning community, a variety of methods have been proposed, which (following [47]) can be mainly organized in three categories: feature based methods, such as subspace mappings [26; 29; 48], finding domain-invariant spaces [59; 30] and optimal transport [22; 21]; inference based methods, including minimax estimators [52; 93; 17] and self-learning [12; 94]; and thirdly, sample based approaches, with a focus on importance weighting [76; 82; 20], mainly in the covariate shift framework, which is our focus.

Covariate Shift: For a model trained on unrepresentative source data to be adapted to accurately predict labels on the target data, information about the target data distribution is required. In this paper, we consider the covariate shift case, a particular case of domain adaptation. Specifically, let $\mathcal{X} \subset \mathbb{R}^F$, $F > 0$, be the feature space and \mathcal{Y} the label space with $K > 1$ classes, or a subset of \mathbb{R}^K in the multivariate regression case with K dependent variables. Different domains are defined as different joint probability distributions $p(x, y)$ over the same feature-label space pair $\mathcal{X} \times \mathcal{Y}$ [47]. We consider a transductive, unsupervised domain adaptation case, where source data $D_S = \{(x_S^{(i)}, y_S^{(i)})\}_{i=1}^{n_s}$ with n_s labelled samples from the joint distribution p_S (source domain \mathcal{D}_S) is available, as well as target data $D_T = \{x_T^{(i)}\}_{i=1}^{n_t}$ with n_t unlabelled samples, from the joint distribution p_T (target domain \mathcal{D}_T). To avoid the simplest case, we assume that $p_S(x, y) \neq p_T(x, y)$. For ease of notation, by writing $p_S(y, x)$ we implicitly condition on a binary indicator variable S , with $p_S(x, y) := p(x, y | s = 1)$ indicating source data selection (analogously $p_T(x, y) := p(x, y | s = 0)$ for target data). Covariate shift is a particular domain adaptation problem, where the conditional distribution of the output variable given the predictive covariates is the same for the source and target data, but the distribution of source and target covariates differ:

Definition 1 ([58]). *Covariate shift is defined as $p_S(y|x) = p_T(y|x)$ but $p_S(x) \neq p_T(x)$.*

In most machine learning tasks, the labeled data does not perfectly represent the unlabeled target data distribution. Covariate shift commonly occurs if the selection (acquisition) of labeled training samples from a pool of unlabeled data is not entirely at random, but biased in terms of certain covariate attributes. The issue of selection bias has been widely studied in the statistical literature [32; 19; 51], e.g., when estimating treatment effects via observational causal inference studies, where the treatment selection is not at random but biased with regards to confounding covariates, associated with both treatment selection and outcome value. The transfer of causal inference techniques to domain adaptation methods has received more attention in recent years [70; 56] – both fields share the goal of obtaining accurate estimators under distribution shift [56; 31].

Propensity scores: The introduction of propensity scores [72; 73] was groundbreaking in the causal inference literature for obtaining unbiased treatment effect estimates from confounded, observational data. [72] define the propensity score as the probability of treatment assignment given the observed covariates. They show that, under certain assumptions, conditional on the propensity scores the treatment and control group have balanced covariates, which allows unbiased average treatment effect estimation. Four methods are mainly used to condition on the propensity scores in the causal inference literature: inverse probability of treatment weighting (IPTW), using the propensity score for covariate adjustment, matching, and stratification on the propensity scores [72; 73; 71; 36]. Much work has been expended towards best-practice and generalization of the propensity score methodology in the causal inference framework [35; 55; 4], which has also found wide application to areas such as classification with imbalanced classes [69], unbiased learning-to-rank and evaluation of recommender systems [40; 74], fairness-aware machine learning [14], and learning from positive and unlabeled data [6]. In the covariate shift framework, estimated propensity scores are implicitly utilized for importance weighting, e.g. [96] and [42], analogously to IPTW. Recently, [16] use propensity score matching to obtain validation data for hyperparameter selection to improve predictive uncertainty of a Bayesian Neural Network under covariate shift.

Contribution: In this paper, we propose stratified learning (*StratLearn*), a novel and statistically principled framework to improve statistical machine learning under covariate shift, based on propensity score stratification. More precisely, we partition (stratify) the (source and target) data into several subgroups conditional on the estimated propensity scores, leading to balanced covariates within strata. We show that the supervised learning models can then be optimized within the source strata without further adjustment, leading to reduced bias in the predictions for each stratum. Our method is general-purpose, meaning it is in principle applicable to any supervised regression or classification task under any model. We provide theoretical evidence for our approach, and we demonstrate its effectiveness on a range of low and high dimensional toy and real-life data applications. Our approach is computationally efficient, easy to implement and readily adaptable to various data applications.

We first illustrate our approach on a well-known univariate regression example [76], and then demonstrate its effectiveness on two topical research issues in modern astronomy. Type Ia supernovae (SNIa) are invaluable for the study of the accelerated expansion of the universe [68; 63]. Identification of SNIa based on time-series observations of their light in various color bands, i.e., photometric

light-curve (LC), has attracted broad interest in recent years, leading to several public classification challenges based on simulated LC data [45; 44; 3] and various proposed classification approaches [53; 66; 10; 91; 11; 57]. We demonstrate that *StratLearn* improves upon the method proposed by [66], on which the winning algorithm [10] of the most recent classification challenge was based. We further improve upon existing non-parametric full conditional density estimation of galaxy redshift [38].¹ Our investigations suggest that our method is competitive to state-of-the-art importance weighting methods on low-dimensional data, and greatly advantageous on higher-dimensional applications.

2 Preliminaries – Learning under covariate shift

Problem Definition – Target Risk Minimization: In a supervised learning task, let $f : \mathcal{X} \rightarrow \mathbb{R}^K$ be the training function, with f an element of the hypothesis space \mathcal{H} . (This describes a general multivariate regression case; in a probabilistic classification task with K classes we usually have $f : \mathcal{X} \rightarrow [0, 1]^K$.) Further, let $\ell : \mathbb{R}^K \times \mathcal{Y} \rightarrow [0, \infty)$ be the training loss function comparing the output of f with the true outcome \mathcal{Y} , and $\mathcal{R}(f) := \mathbb{E}[\ell(f(x), y)]$ the risk function associated to our supervised learning task. We cannot generally compute $\mathcal{R}(f)$, since the exact joint distribution $p(x, y)$ is unknown in practice. However, an approximation of the risk can be obtained by computing the empirical risk by averaging the loss on the training sample [24].

In the covariate shift framework, the objective is to minimize the target risk $\mathcal{R}_T(f)$, defined as the expected target loss $\mathcal{R}_T(f) := \mathbb{E}_{(x, y) \sim p_T(x, y)}[\ell(f(x), y)]$, via the labelled source data \mathcal{D}_S and unlabelled target data \mathcal{D}_T . Loosely speaking, our goal is to train a model function f that minimizes $\mathcal{R}_T(f)$ while being able to compute the source loss $\ell(f(x_S), y_S)$, but not the target loss $\ell(f(x_T), y_T)$.

Related Literature – Importance weighting: In an influential work, [76] proposes a weighted maximum likelihood estimation (MWLE) and shows that this MWLE converges in probability to the minimizer of the target risk. Proposition 1 presents a generalization of this weighting approach.

Proposition 1 ([76], [8]). *If the support of $p_T(x)$ is contained in $p_S(x)$, the expected loss (risk) w.r.t. \mathcal{D}_T equals that w.r.t. \mathcal{D}_S with weights $w(x) = p_T(x)/p_S(x)$ for the loss incurred by each x ,*

$$\mathbb{E}_{(x, y) \sim \mathcal{D}_T} [\ell(f(x), y)] = \mathbb{E}_{(x, y) \sim \mathcal{D}_S} \left[\frac{p_T(x)}{p_S(x)} \ell(f(x), y) \right]. \quad (1)$$

In short, the target risk can be minimized by weighting the source domain loss by a ratio of the densities of target and source domain features, respectively. The importance weights $w(x)$ in Proposition 1 are central in the covariate shift literature and several approaches have been proposed to optimize the estimation of the weights. A possible approach is to estimate the densities separately [76], e.g. through kernel density estimators [81; 95; 5]. Much research has been done to estimate the density ratio directly, such as Kernel-Mean-Matching in a reproducing kernel Hilbert space [34; 92], Kullback-Leibler importance estimation (KLIEP) [82; 86], and variations of unconstrained least-squares importance fitting (uLSIF) [42; 43; 87]. Given the importance weights $w(x)$, [80] propose an importance weighted k-fold cross-validation (IWCV) and show that in theory this can deliver an almost unbiased estimate of the target risk. [96] links covariate shift with selection bias.

Proposition 2 (Bias Correction [96]). *Let (x, y, s) be examples drawn from a distribution \mathcal{D} , with feature-label-selection space $\mathcal{X} \times \mathcal{Y} \times \mathcal{S}$. For any distribution \mathcal{D} , for all classifiers f , and for any loss function $\ell = \ell(f(x), y)$, if we assume that $P(s = 1|x, y) = P(s = 1|x)$, then*

$$\mathbb{E}_{(x, y) \sim \mathcal{D}} [\ell(f(x), y)] = \mathbb{E}_{(x, y) \sim \hat{\mathcal{D}}} [\ell(f(x), y) | s = 1], \quad (2)$$

$$\text{with } \hat{\mathcal{D}}(x, y, s) := \frac{P(s = 1)}{P(s = 1|x)} \mathcal{D}(x, y, s). \quad (3)$$

The target risk can thus be minimised by sampling $\hat{\mathcal{D}}$, e.g., by importance sampling of source domain data. Formula (3) allows us to use any probabilistic classifier to estimate the probabilities $P(s = 1|x)$, e.g., logistic regression [9].

Even though in theory such importance weighting schemes enable the minimization of the target risk, they are subject to several challenges. Based on a measure of domain dissimilarity (e.g., Rényi

¹Additional numerical evidence is provided in the Supplement on data from the UCI repository [25], and on a variation of the SPCC data [45].

divergence [88]), [20] show that the weighting schemes lead to high generalization upper error bounds, thus making the predictions unreliable, especially for large importance weights. In addition, [65] points out that while weighting can reduce bias, it can also greatly increase variance, and thus [65] proposes a doubly-robust covariate shift correction. Unfortunately, with increasing dimensionality of the feature space, the variance of the importance weighted empirical risk estimates might increase [37; 78]. This can be partly tackled by dimensionality reduction methods, e.g. [83]. We refer to [60; 47] for a more detailed discussion of prior work.

3 Methodology – Covariate Shift adjustment through Stratified Learning

Recall that in the covariate shift framework we have source data x_S with labels y_S and target data x_T . In this context, we define the propensity score to be the probability that object i is selected in the source data, given all observed covariates and samples from source and target, i.e.,

$$e(x_i) := P(s_i = 1 | x_S, x_T), \text{ with } 0 < e(x_i) < 1. \quad (4)$$

Proposition 3 (Learning conditional on the propensity score²). *If $p_S(x, y)$ and $p_T(x, y)$ satisfy the definition of covariate shift and $0 < e(x) < 1$, then it holds that*

$$p_T(x, y | e(x)) = p_S(x, y | e(x)). \quad (5)$$

That is, conditional on the propensity score $e(x)$ the joint source and target distributions are the same, eliminating the covariate shift. It directly follows, for any loss function $\ell = \ell(f(x), y)$, that

$$E_{(x,y) \sim p_T(x,y|e(x))}[\ell(f(x), y)] = E_{(x,y) \sim p_S(x,y|e(x))}[\ell(f(x), y)]. \quad (6)$$

According to Proposition 3, if we were to condition on any single value of the propensity score, the distribution of x and y in the source and target domains with this value would be identical and we could minimize their target risk using the source data alone. Because data subsets with identical propensity scores are too small in practice for model fitting, we must employ some approximation.

StratLearn takes advantage of Proposition 3 via propensity score stratification; source data D_S and target data D_T are divided into k non-overlapping subgroups (strata) based on the quantiles of the estimated propensity scores. More precisely, for $j \in 1, \dots, k$, we divide D_S and D_T into

$$D_{Sj}^{(k)} = \{(x, y) \in D_S : q_{k-j} < e(x) \leq q_{k-j+1}\} \text{ and } D_{Tj}^{(k)} = \{x \in D_T : q_{k-j} < e(x) \leq q_{k-j+1}\}, \quad (7)$$

where q_j is the j 'th k -quantile of $\{e(x_i) : x_i \in (x_S \cup x_T)\}$ and $q_0 = 0, q_k = 1$. As a consequence of Proposition 3, by conditioning on the estimated propensity scores via stratification [72; 73], we have

$$p_{Tj}(y, x) \approx p_{Sj}(y, x), \text{ for } j \in 1, \dots, k, \quad (8)$$

where the subscript S_j means that we condition on assignment to the j 'th source stratum (analogously for target T_j). It directly follows that

$$\mathbb{E}_{(x,y) \sim p_{Tj}(x,y)}[\ell(f(x), y)] \approx \mathbb{E}_{(x,y) \sim p_{Sj}(x,y)}[\ell(f(x), y)], \text{ for } j \in 1, \dots, k. \quad (9)$$

This means that we can minimize the target risk in a stratum by minimizing the source risk in that stratum. In this way, we reduced the covariate shift problem to non-overlapping subgroups where the source and the target domain are approximately the same, which in principle allows us to fit any supervised learner to the source data D_{Sj} and predict on the target objects in D_{Tj} .

Technical details: Logistic regression is commonly used to estimate propensity scores in the causal inference literature, and we find it adequate for the applications provided here. In practice, the covariate shift assumption, $p_S(y|x) = p_T(y|x)$, requires that there are no unobserved confounding covariates. To meet this requirement, we include all suspected confounders as main effects in the logistic-regression propensity-score estimation model. Based on the estimated propensity scores, the source and target data are then grouped into strata, following (7). Thus, the first stratum contains samples more likely from the source distribution, and the upper strata contain samples less likely

²Proposition 3 is verified in the Supplement. Its condition, $0 < e(x) < 1$, is no stronger than the general conditions in Section 2. The support of $p_T(x)$ being contained in $p_S(x)$ implies $0 < e(x)$, and $e(x) = 1$, would mean $p_T(x) = 0$, in which case the importance weight, $w(x) = 0$, which is equivalent to discarding the sample.

from the source data distribution. We use $k = 5$ strata based on empirical evidence provided by [18], showing that sub-grouping into five strata is enough to remove at least 90 percent of the bias for many continuous distribution [72]. Given the stratified data, we fit a model f_j to source data D_{S_j} , and predict the respective target samples in D_{T_j} , for $j \in 1, \dots, k$. Model hyperparameters for f_j can be selected through empirical risk minimization on source data D_{S_j} , for instance through cross-validation on D_{S_j} . The model functions f_j are trained independently and can thus be computed in parallel to reduce computation time. When higher strata have insufficient source data for model training, we add source data from one or more adjacent stratum/strata for training (see, e.g., Sections 4.2 and 4.3).

4 Demonstration

4.1 Comparison Models

We compare *StratLearn* to a range of well-established importance weighting methods.

- KLIEP – Kullback-Leibler Importance estimation procedure, minimizing the KL-divergence between the target distribution and weighted source distribution [82].
- uLSIF – unconstrained least-squares importance fitting, minimizing the L2-norm as domain discrepancy [42].³
- NN – We examined several versions of the Nearest-Neighbor (NN) importance weight estimator [50; 49; 54], varying the selected number of neighbors.
- IPS – The importance weights are estimated through probabilistic classification of source set assignment [42], (precise description in the Supplement, Formula (17)). We call this method IPS because it directly incorporates the Inverses of the estimated Propensity Scores.

In the following sections, the estimated weights are incorporated as in the respective benchmark examples [76; 38]. Specifically, in Section 4.2 the estimated weights are used for importance weighted least squares regression [76]. In Section 4.4, following [38] the estimated weights are used for loss weighting (Proposition 1). In Section 4.3, importance weighting has not previously been applied. We implement importance weighted cross-validation [80], importance sampling (Proposition 2), and a combination of both, to demonstrate the superior performance of *StratLearn* to either approach.

4.2 Regression – Univariate example

We first illustrate *StratLearn* on a well known univariate example from [76]. Source data is simulated with $X_S \sim N(\mu_S = 0.5, \tau_S^2 = 0.5^2)$ and target data with $X_T \sim N(\mu_T, \tau_T^2)$, independently. We investigate three different target parameter settings:

- (i) $\mu_T = 0, \tau_T = 0.3$ (ii) $\mu_T = 0, \tau_T = 0.5$ (iii) $\mu_T = 0.2, \tau_T = 0.5$,

where example (i) replicates the target parameters from [76], and examples (ii) and (iii) are variations of (i) to illustrate robustness to the degree of covariate shift. In all three examples, the continuous outcome is simulated as a polynomial with degree $d = 3$, specifically as $y = -x + x^3 + \epsilon$, with $\epsilon \sim N(0, 0.3^2)$. We assume that 100 independent samples are observed from each of X_S and X_T , along with the source outcome (blue circles in Figure (1)), with the aim of predicting the target outcome (black triangles). Following [76], we fit a misspecified (linear) model ($d = 1$).

To compare the performance of *StratLearn* to an ordinary least squares model (OLS) and weighted least squares (WLS) [76], we evaluated each model on $m = 1000$ replicate data sets, each simulated as described above. Importance weights for WLS are estimated using the models described in Section 4.1. In addition, since the density of the target and source data are known in this case, [76] computes the weights analytically as the ratio of the two normal densities $w(x) = N(\mu_T, \tau_T^2)/N(\mu_S, \tau_S^2)$. We assessed the performance of the models by the mean squared error (MSE) of the predictions of the target data in each of the $m = 1000$ data sets as summarized in the boxplots in Figure 1.

We implement *StratLearn* following the principles described in Section 3, by splitting the data into five equally sized strata based on logistic-regression estimated propensity scores, and fitting ordinary least squares on the source data within each stratum to predict the target outcome within

³KLIEP and uLSIF were implemented with the original author’s public domain MATLAB code (link).

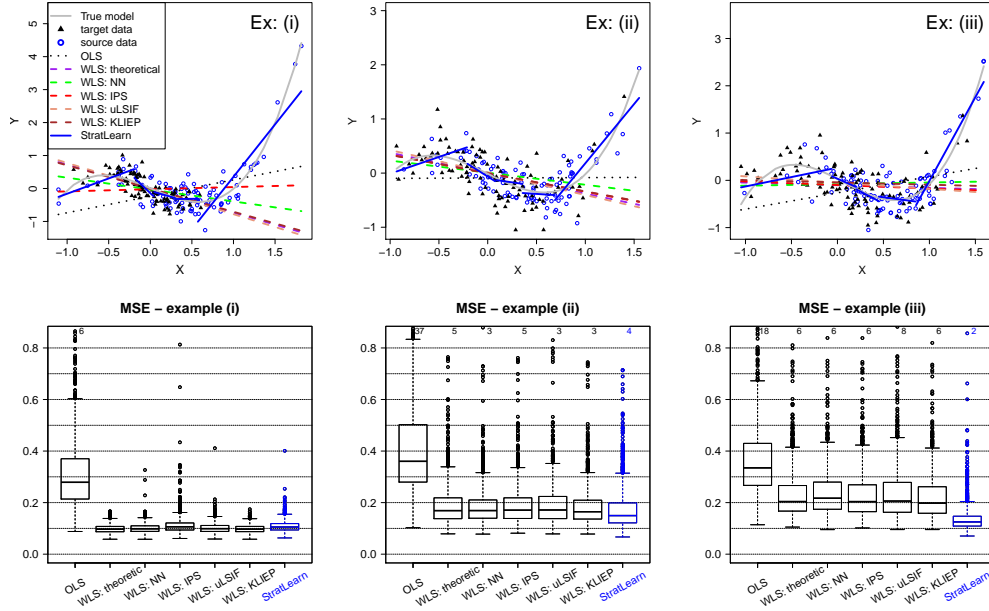


Figure 1: Top: Representative fit for each of the target parameter setting (i)-(iii). Bottom: Boxplot of the target MSE, obtained by fitting the models on $m = 1000$ Monte Carlo simulations; examples (i) to (iii) from left to right. The small numbers at the top are the number of outliers beyond the limit of the graph. Mean and standard error of the MSE are in the Supplement.

the respective stratum. Sample fits of *StratLearn* are shown in Figure (1) for examples (i)-(iii) (blue lines), illustrating that *StratLearn* approximates well the true data generation model (grey line). To ensure that there is enough source data in the last stratum, the source data from stratum 4 was added to fit the model for stratum 5 in cases where replicate data had fewer than 10 source samples in stratum 5. Using a minimum threshold of 5 source samples led to very similar model performance (Supplement, Figure 4), demonstrating robustness with respect to the choice of this threshold.

In summary, *StratLearn* led to substantially lower MSE (averages: 0.108, 0.181, 0.140) than the OLS method (0.312, 0.415, 0.370) in all three examples. In example (ii), and especially in example (iii), *StratLearn* led to the lowest errors across all compared models. In example (i) the theoretical weights and the KLIEP estimated weights led to the lowest mean MSE (0.098), whereas *StratLearn* still led to lower mean MSE than the IPS importance weighting method. The MSE boxplot ranges in this example strongly overlap between *StratLearn* and the WLS methods.

4.3 Classification – Supernova photometric classification challenge

Objective: Reliable identification of supernovae Type Ia (SNIa) based on photometric light curve (LC) data is a major issue in modern observational cosmology. Photometric LC data is easily collectable, consisting of measurements of an astronomical object’s brightness, filtered through different passbands (wavelength ranges), at a sequence of time points. Only a small subset of the objects are labelled via time-intensive spectroscopical observations. The labeled source data D_S is not representative of the photometric target data D_T , as the selection of spectroscopic source samples is biased towards higher brightness and bluer objects. Much effort has been expended to provide automatic classification of photometric (unlabelled) objects (target data), based on biased spectroscopically confirmed source data [45; 46; 3; 66; 53; 10].

Leading SNIa classification approaches are based on data augmentation by sampling synthetic objects from Gaussian process (GP) fits of the LCs to overcome covariate shift [66; 10]. The method proposed by [66] (“STACCATO”) can be viewed as a prototype of *StratLearn*, as it augments the source data separately in strata based on the estimated propensity scores. However, to optimize the augmentation of the data in each stratum, [66] require a sub-sample of labeled target data, not available in practice.

While effective in this particular case, GP data augmentation is generally not an option in most covariate shift tasks. Building upon the approach by [66], we show that principled application of *StratLearn* makes augmentation dispensable for binary classification of SNIa vs. non-SNIa, using a random forest classifier as proposed in [66]. For comparison to previously published methods, the predictive performance is measured by the target prediction AUC.

Data and preprocessing We use data from the updated “Supernova photometric classification challenge” (SPCC) [44], containing a total of 21,318 simulated SNIa and of other types (Ib, Ic and II). For each supernova (SN), LCs are given in four color bands, $\{g, r, i, z\}$. The data is divided into a source (training) set D_S of 1102 spectroscopically confirmed SNe with known types and 20,216 SNe with unknown types (target set D_T). 51% of the source objects are of type Ia, while only 23% are of type Ia in the target data, a consequence of the strong covariate shift in the data.

We follow the approach in [66], which has been applied to an earlier release of the SPCC data [45] (discussed in the Supplement), to extract a set of features from the LC data that can be used for classification. First, a GP with a squared exponential kernel is used to model the LCs. Then, a diffusion map [67] is applied, resulting in a vector of similarity measures between the LCs that can be used as predictor variables. We thus obtain 102 predictive covariates, 100 covariates from the diffusion map, plus redshift (defined in Section 4.4) and a measure of the objects’ brightness [66].

Results: First, we evaluate the impact of covariate shift on classification by training a random forest classifier on the source covariates ignoring covariate shift, resulting in an AUC of 0.902 on the target data (black ROC curve in Figure 2). Next, we obtain a ‘gold standard’ benchmark by randomly selecting 1,102 samples from the combined source and target data as representative source set. Applying the same classification procedure on this unbiased ‘gold standard’ training data (unavailable in practice), we obtain an AUC of 0.965 on the 20,216 test samples.

Given the biased source data, *StratLearn* is implemented as described in Section 3, including all 102 covariates in the logistic propensity score estimation model. The improved covariate balance within strata is discussed and illustrated in the Supplement. After stratification, a random forest classifier is trained and optimized on source strata D_{S_1} and D_{S_2} separately to predict samples in target strata D_{T_1} and D_{T_2} . We used repeated 10-fold cross validation with a large hyperparameter grid to minimize the empirical risk of (9) within each strata; details appear in the Supplement. Source strata D_{S_j} for $j \in \{3, 4, 5\}$ have a small sample size, (13,7,4) respectively. Thus, the source strata are merged with D_{S_2} to train the random forest to predict D_{T_j} for $j \in \{3, 4, 5\}$. With *StratLearn*, we obtain an AUC of 0.958 on the target data (blue ROC curve in Figure 2), very near the optimal ‘gold standard’ benchmark.

Figure 2 compares *StratLearn* to importance sampling methods designed to adjust for covariate shift (Proposition 2). To perform importance sampling in this example, the bootstrapped samples in the random forest fit were resampled with probabilities proportional to the estimated importance weights (details provided in the Supplement). NN and IPS led to the best importance weighted classifier with an AUC of 0.923 and 0.921, respectively – an improvement over the biased fit, but still substantially lower than *StratLearn*. KLIEP failed to fit importance weights in this example and is thus not included in the results. We also implemented importance weighted cross validation (IWCV) [80], using the same hyperparameter grid as for *StratLearn*, and a combination of IWCV and importance sampling, which both led to lower AUC than the ones reported in Figure 2 (numerical results are presented in the Supplement).

Previous state-of-the-art approaches obtain an AUC of 0.855 [53] using boosted decision trees, 0.939 [61] using a combined framework of an autoencoder and a convolutional neural network and 0.94 [66], using LC augmentation and target data leakage, all lower than *StratLearn*.

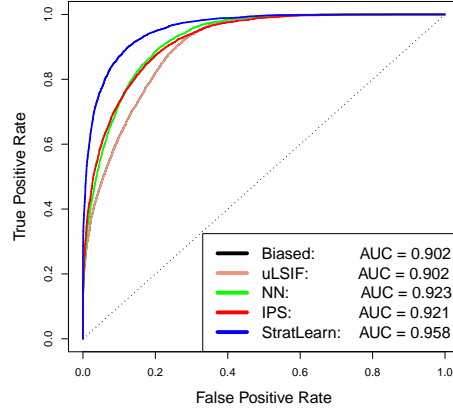


Figure 2: Comparison of ROC curves for SNIa classification using the updated SPCC data. Here, Biased and uLSIF are identical.

4.4 Full conditional density estimation – Photometric redshift regression

Objective: The wavelength of light from extragalactic objects is stretched because of the expansion of the universe – a phenomenon called ‘redshift’. This fractional shift towards the red end of the spectrum is denoted by z , and its accurate quantification is essential for cosmological inference. Because of instrumental limitations, redshift can be precisely measured for a small fraction of the $\sim 10^7$ galaxies observed to date (set to grow to $\sim 10^9$ within a decade). This source data is subject to covariate shift relative to the set of galaxies with unknown redshift (target). References [38; 27] employed importance weighting to adjust for covariate shift in x , a set of observed photometric magnitudes (a logarithmic measure of passband-filtered brightness), when estimating z . They obtain a non-parametric estimate of the conditional density, $f(z|x)$, to quantify predictive uncertainty of redshift estimates. Using the same setup and conditional density estimators (hist-NN, ker-NN, Series and Comb, detailed in [38]),⁴ we show that *StratLearn* leads to better predictive performance than importance weighting.

Specifically, we follow [38], and optimize the importance weighted conditional density estimators with respect to a *generalized* risk (generalized in that the underlying loss can be negative):

$$\hat{R}_S(\hat{f}) = \frac{1}{n_T} \sum_{k=1}^{n_T} \int \hat{f}^2(z|x_T^{(k)}) dz - 2 \frac{1}{n_S} \sum_{k=1}^{n_S} \hat{f}(z_S^{(k)}|x_S^{(k)}) \hat{w}(x_S^{(k)}), \quad (10)$$

where the weights, $\hat{w}(x_S) = p_T(x)/p_S(x)$, are estimated using the models in Section 4.1. As their best performing model, [38] propose an average of importance weighted ker-NN and Series,

$$\hat{f}^\alpha(z|x) = \sum_{k=1}^p \alpha_k \hat{f}_k(z|x), \text{ with constraints (i): } \alpha_i \geq 0, \text{ and (ii): } \sum_{k=1}^p \alpha_k = 1, \quad (11)$$

referred to as ‘Comb’ (i.e., combination), where $p = 2$ and α_i is optimized to minimize (10).

With *StratLearn*, we minimize (10) in each source stratum separately (with $w(x) \equiv 1$). We propose a *StratLearn* version of Comb by optimizing (11) on each source stratum separately (with $w(x) \equiv 1$), including ker-NN and Series (each optimized via *StratLearn* beforehand). This and the other methods are compared with a “Biased” fit that simply fixes $w(x) \equiv 1$.

Data: We use the same data set as [38], consisting of 467,710 galaxies from [75; 2], each with spectroscopic redshift z (measured with negligible error), and five photometric covariates x . We denote this spectroscopic source sample by D_S . To simulate realistic covariate shift, we follow [38]: starting from D_S , we use rejection sampling to simulate a photometric, unrepresentative target sample D_T , with the prescription $p(s = 0|x) = f_{B(13,4)}(x_{(r)})/\max_{x_{(r)}} f_{B(13,4)}(x_{(r)})$, where $x_{(r)}$ is the r -band magnitude and $f_{B(13,4)}$ is a beta density with parameters (13,4). Additionally, we investigated adding $k \in \{10, 50\}$ i.i.d. standard normal covariates as potential predictors to the 5 photometric covariates. This simulates the realistic case where additional potentially confounding covariates might be present. For comparability, we follow [38] and use $|D_S^{\text{train}}| = 2800$ galaxies randomly sampled from D_S as our training data, plus a validation set of $|D_S^{\text{val}}| = 1200$ galaxies. We assess predictive performance of the models using a random subset of D_T , i.e., $|D_T^{\text{test}}| = 6000$.

Results: For the final evaluation of \hat{f} under the various models, we use the known target redshifts, z_T , to compute the target risk, $\hat{R}_T(\hat{f})$, via a non-weighted version of (10) with $x_S^{(k)}$ and $y_S^{(k)}$ replaced by $x_T^{(k)}$ and $y_T^{(k)}$. Figure 3 compares the resulting target risk \hat{R}_T across models and covariate sets, showing that *StratLearnComb* gives the best performance in all three covariate setups.

For small covariate space dimension (Fig 3, left panel), *StratLearnComb* improves upon *StratLearnker-NN* and *StratLearnSeries*, optimizing the source risk in each stratum separately and combining their predictions. In the presence of potential additional confounding covariates (Fig 3, middle and right panels), *StratLearnComb* exploits the higher performance of *StratLearnker-NN*, given that *StratLearnSeries* suffers from poor target performance in these cases. In contrast, for the non-adjusted (Biased) and importance weighted models the combination of approaches (‘Comb’) does

⁴For the computation of the conditional density estimators we used data (provided to us with consent by the authors of [75]) and code (via Project Euclid) by [38] (link).

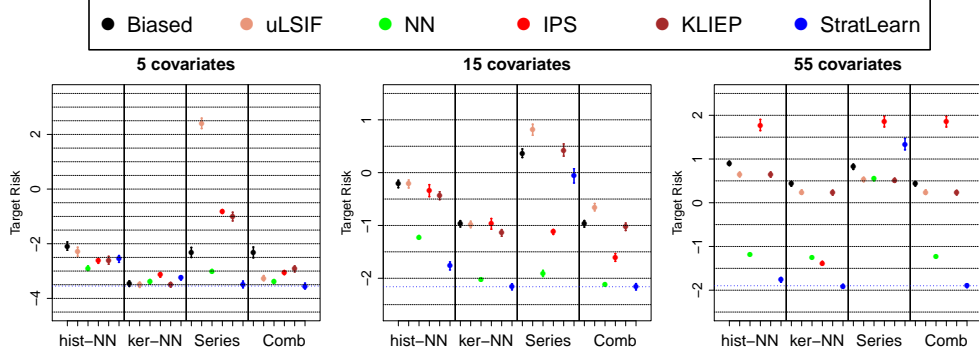


Figure 3: Target risk (R_T) of photometric redshift estimation models, using different sets of predictors. Bars give the mean ± 2 bootstrap standard errors (from 400 bootstrap samples).

not necessarily lead to increased performance (e.g., $\text{Biased}_{\text{Comb}}$ features a higher target risk than $\text{Biased}_{\text{ker-NN}}$ on its own). The improvement of *StratLearn* relative to other methods increases with the dimensionality of the covariate space. In particular, the performance of nearest neighbour-based methods, which is competitive in low dimensions, rapidly degrades in higher (noisy) covariate dimensions, in contrast to the more robust *StratLearn*.

5 Discussion – Conclusion, Limitation and Future Direction

Limitations and societal impact: This paper demonstrated a statistically principled methodology to obtain accurate, robust and reliable predictions for target data suffering from systematic differences relative to the source data in terms of covariate distributions. Covariate shift is a common and pernicious issue in many supervised learning tasks, both in fundamental science and in applied fields. Our method has potential applications in improving decision-making with major societal impact, e.g. automated recruitment procedures, loan approvals, recommender systems, and healthcare decisions, among others. Automated learning schemes have been shown to suffer from e.g., gendered stereotyping from language corpora [15], differential performance (e.g., in facial recognition [13]) and systematic discrimination (e.g., in re-offending prediction [77]). Some of these flaws are a consequence of unbalanced features such as gender, ethnicity, age, etc. in the training data, leading to representation, measurement and aggregation bias, in the terminology of [84]. While our approach provides a route to mitigating or eliminating entirely such bias by balancing covariates within strata, it remains a limited technical solution, which by itself cannot claim to obtain fairness in prediction for such applications. Also, the assumption of covariate shift is rather strong, requiring that there are no unmeasured confounding covariates – something that cannot be guaranteed in general. In the Supplement we demonstrate a certain robustness of our method against violation of this assumption, yet further work is necessary to assess more fully the performance of *StratLearn* when this assumption is only approximately fulfilled. In its current form, our method does not investigate multi-class classification. While *StratLearn* can in principle be extended to such a case, the availability of a sufficiently large source sample from each class in each stratum may become a challenge.

Conclusion: We provide a novel framework for learning under covariate shift, theoretically justified and based on principles derived in the propensity score causal inference framework [72]. We show that *StratLearn* outperforms a range of state-of-the-art importance weighting methods both on toy covariate shift examples and on contemporary research questions in cosmology, especially in the presence of a high dimensional covariate space. We emphasize that the covariate shift framework is best justified in the presence of a large number of covariates mitigating the risk of unmeasured confounders – in which case it is critical to adopt a method that, like *StratLearn*, can robustly handle many covariates. Our framework is entirely general and versatile, as demonstrated with examples of regression, conditional density estimation and classification, and dispenses with the need for data

augmentation. We believe it may become a powerful alternative to importance weighting, with a myriad of possible extensions and applications.

Acknowledgments and Disclosure of Funding

Roberto Trotta’s work was partially supported by STFC under grant number ST/P000762/1 and ST/T000791/1 and David Stenning acknowledges the support of the Natural Sciences and Engineering Research Council of Canada (NSERC), RGPIN-2021-03985. Finally, the authors acknowledge support from the Marie-Skłodowska-Curie RISE (H2020-MSCA-RISE-2019-873089) Grant provided by the European Commission.

References

- [1] Agarwal, D., Li, L., and Smola, A. (2011), “Linear-time estimators for propensity scores,” in *Proceedings of the Fourteenth International Conference on Artificial Intelligence and Statistics*, pp. 93–100.
- [2] Aihara, H., Prieto, C. A., An, D., Anderson, S. F., Aubourg, É., Balbinot, E., Beers, T. C., Berlind, A. A., Bickerton, S. J., Bizyaev, D. et al. (2011), “The eighth data release of the Sloan Digital Sky Survey: first data from SDSS-III,” *The Astrophysical Journal Supplement Series*, 193, 29.
- [3] Allam Jr, T., Bahmanyar, A., Biswas, R., Dai, M., Galbany, L., Hložek, R., Ishida, E. E., Jha, S. W., Jones, D. O., Kessler, R. et al. (2018), “The photometric lsst astronomical time-series classification challenge (plasticc): Data set,” *arXiv preprint arXiv:1810.00001*.
- [4] Austin, P., and Stuart, E. (2015), “Moving towards best practice when using inverse probability of treatment weighting (IPTW) using the propensity score to estimate causal treatment effects in observational studies,” 34.
- [5] Baktashmotlagh, M., Harandi, M. T., Lovell, B. C., and Salzmann, M. (2014), “Domain adaptation on the statistical manifold,” in *Proceedings of the IEEE conference on computer vision and pattern recognition*, pp. 2481–2488.
- [6] Bekker, J., Robberechts, P., and Davis, J. (2019), “Beyond the selected completely at random assumption for learning from positive and unlabeled data,” in *Joint European Conference on Machine Learning and Knowledge Discovery in Databases*, Springer, pp. 71–85.
- [7] Ben-David, S., Blitzer, J., Crammer, K., Kulesza, A., Pereira, F., and Vaughan, J. W. (2010), “A theory of learning from different domains,” *Machine learning*, 79, 151–175.
- [8] Bickel, S., Brückner, M., and Scheffer, T. (2009), “Discriminative learning under covariate shift,” *Journal of Machine Learning Research*, 10, 2137–2155.
- [9] Bickel, S.— (2007), “Dirichlet-enhanced spam filtering based on biased samples,” in *Advances in neural information processing systems*, pp. 161–168.
- [10] Boone, K. (2019), “Avocado: Photometric classification of astronomical transients with gaussian process augmentation,” *The Astronomical Journal*, 158, 257.
- [11] Brunel, A., Pasquet, J., Pasquet, J., Rodriguez, N., Comby, F., Fouchez, D., and Chaumont, M. (2019), “A CNN adapted to time series for the classification of Supernovae,” *Electronic Imaging*, 2019, 90–1.
- [12] Bruzzone, L., and Marconcini, M. (2009), “Domain adaptation problems: A DASVM classification technique and a circular validation strategy,” *IEEE transactions on pattern analysis and machine intelligence*, 32, 770–787.
- [13] Buolamwini, J., and Gebru, T. (2018), “Gender shades: Intersectional accuracy disparities in commercial gender classification,” in *Conference on fairness, accountability and transparency*, PMLR, pp. 77–91.

- [14] Calders, T., Karim, A., Kamiran, F., Ali, W., and Zhang, X. (2013), “Controlling attribute effect in linear regression,” in *2013 IEEE 13th international conference on data mining*, IEEE, pp. 71–80.
- [15] Caliskan, A., Bryson, J. J., and Narayanan, A. (2017), “Semantics derived automatically from language corpora contain human-like biases,” *Science*, 356, 183–186.
- [16] Chan, A., Alaa, A., Qian, Z., and Van Der Schaar, M. (2020), “Unlabelled data improves bayesian uncertainty calibration under covariate shift,” in *International Conference on Machine Learning*, PMLR, pp. 1392–1402.
- [17] Chen, X., Monfort, M., Liu, A., and Ziebart, B. D. (2016), “Robust covariate shift regression,” in *Artificial Intelligence and Statistics*, PMLR, pp. 1270–1279.
- [18] Cochran, W. G. (1968), “The effectiveness of adjustment by subclassification in removing bias in observational studies,” *Biometrics*, 295–313.
- [19] Cochran, W. G., and Rubin, D. B. (1973), “Controlling bias in observational studies: A review,” *Sankhyā: The Indian Journal of Statistics, Series A*, 417–446.
- [20] Cortes, C., Mansour, Y., and Mohri, M. (2010), “Learning bounds for importance weighting,” in *Advances in neural information processing systems*, pp. 442–450.
- [21] Courty, N., Flamary, R., Habrard, A., and Rakotomamonjy, A. (2017), “Joint distribution optimal transportation for domain adaptation,” *arXiv preprint arXiv:1705.08848*.
- [22] Courty, N., Flamary, R., Tuia, D.— (2016), “Optimal transport for domain adaptation,” *IEEE transactions on pattern analysis and machine intelligence*, 39, 1853–1865.
- [23] Csúrká, G. (2017), “A comprehensive survey on domain adaptation for visual applications,” *Domain adaptation in computer vision applications*, 1–35.
- [24] Devroye, L., Györfi, L., and Lugosi, G. (2013), *A probabilistic theory of pattern recognition*, vol. 31, Springer Science & Business Media.
- [25] Dua, D., and Graff, C. (2017), “UCI Machine Learning Repository,” .
- [26] Fernando, B., Habrard, A., Sebban, M., and Tuytelaars, T. (2013), “Unsupervised visual domain adaptation using subspace alignment,” in *Proceedings of the IEEE international conference on computer vision*, pp. 2960–2967.
- [27] Freeman, P. E., Izbicki, R., and Lee, A. B. (2017), “A unified framework for constructing, tuning and assessing photometric redshift density estimates in a selection bias setting,” *Monthly Notices of the Royal Astronomical Society*, 468, 4556–4565.
- [28] Gieseke, F., Polsterer, K. L., Thom, A., Zinn, P., Bomann, D., Dettmar, R.-J., Kramer, O., and Vahrenhold, J. (2010), “Detecting quasars in large-scale astronomical surveys,” in *2010 Ninth International Conference on Machine Learning and Applications*, IEEE, pp. 352–357.
- [29] Gong, B., Grauman, K., and Sha, F. (2013), “Reshaping visual datasets for domain adaptation,” *Advances in Neural Information Processing Systems*, 26, 1286–1294.
- [30] Gong, M., Zhang, K., Liu, T., Tao, D., Glymour, C., and Schölkopf, B. (2016), “Domain adaptation with conditional transferable components,” in *International conference on machine learning*, PMLR, pp. 2839–2848.
- [31] Hassanpour, N., and Greiner, R. (2019), “Counterfactual regression with importance sampling weights,” in *Proceedings of the Twenty-Eighth International Joint Conference on Artificial Intelligence, IJCAI-19*, pp. 5880–5887.
- [32] Heckman, J. J. (2014), *Sample selection bias as a specification error with an application to the estimation of labor supply functions*, Princeton University Press.
- [33] Hoffman, J., Wang, D., Yu, F., and Darrell, T. (2016), “Fcns in the wild: Pixel-level adversarial and constraint-based adaptation,” *arXiv preprint arXiv:1612.02649*.

- [34] Huang, J., Gretton, A., Borgwardt, K., Schölkopf, B., and Smola, A. J. (2007), “Correcting sample selection bias by unlabeled data,” in *Advances in neural information processing systems*, pp. 601–608.
- [35] Imai, K., and Van Dyk, D. A. (2004), “Causal inference with general treatment regimes: Generalizing the propensity score,” *Journal of the American Statistical Association*, 99, 854–866.
- [36] Imbens, G. W., and Rubin, D. B. (2015), *Causal inference in statistics, social, and biomedical sciences*, Cambridge University Press.
- [37] Izbicki, R., Lee, A., and Schafer, C. (2014), “High-dimensional density ratio estimation with extensions to approximate likelihood computation,” in *Artificial Intelligence and Statistics*, PMLR, pp. 420–429.
- [38] Izbicki, R., Lee, A. B., Freeman, P. E. et al. (2017), “Photo-z estimation: An example of nonparametric conditional density estimation under selection bias,” *The Annals of Applied Statistics*, 11, 698–724.
- [39] Jiang, J., and Zhai, C. (2007), “Instance weighting for domain adaptation in NLP,” ACL.
- [40] Joachims, T., Swaminathan, A., and Schnabel, T. (2017), “Unbiased learning-to-rank with biased feedback,” in *Proceedings of the Tenth ACM International Conference on Web Search and Data Mining*, ACM, pp. 781–789.
- [41] Kamnitsas, K., Baumgartner, C., Ledig, C., Newcombe, V., Simpson, J., Kane, A., Menon, D., Nori, A., Criminisi, A., Rueckert, D. et al. (2017), “Unsupervised domain adaptation in brain lesion segmentation with adversarial networks,” in *International conference on information processing in medical imaging*, Springer, pp. 597–609.
- [42] Kanamori, T., Hido, S., and Sugiyama, M. (2009), “A least-squares approach to direct importance estimation,” *Journal of Machine Learning Research*, 10, 1391–1445.
- [43] Kanamori, T., Suzuki, T.— (2012), “Statistical analysis of kernel-based least-squares density-ratio estimation,” *Machine Learning*, 86, 335–367.
- [44] Kessler, R., Bassett, B., Belov, P., Bhatnagar, V., Campbell, H., Conley, A., Frieman, J. A., Glazov, A., González-Gaitán, S., Hlozek, R. et al. (2010), “Results from the supernova photometric classification challenge,” *Publications of the Astronomical Society of the Pacific*, 122, 1415.
- [45] Kessler, R., Conley, A., Jha, S., and Kuhlmann, S. (2010), “Supernova photometric classification challenge,” *arXiv preprint arXiv:1001.5210*.
- [46] Kessler, R., Narayan, G., Avelino, A., Bachelet, E., Biswas, R., Brown, P., Chernoff, D., Connolly, A., Dai, M., Daniel, S. et al. (2019), “Models and simulations for the photometric LSST astronomical time series classification challenge (PLAsTiCC),” *Publications of the Astronomical Society of the Pacific*, 131, 094501.
- [47] Kouw, W. M., and Loog, M. (2019), “A review of domain adaptation without target labels,” *IEEE transactions on pattern analysis and machine intelligence*.
- [48] Kouw, W. M., Van Der Maaten, L. J., Krijthe, J. H.— (2016), “Feature-level domain adaptation,” *The Journal of Machine Learning Research*, 17, 5943–5974.
- [49] Kremer, J., Gieseke, F., Pedersen, K. S., and Igel, C. (2015), “Nearest neighbor density ratio estimation for large-scale applications in astronomy,” *Astronomy and Computing*, 12, 67–72.
- [50] Lima, M., Cunha, C. E., Oyaizu, H., Frieman, J., Lin, H., and Sheldon, E. S. (2008), “Estimating the redshift distribution of photometric galaxy samples,” *Monthly Notices of the Royal Astronomical Society*, 390, 118–130.
- [51] Little, R. J., and Rubin, D. B. (2019), *Statistical analysis with missing data*, vol. 793, John Wiley & Sons.

- [52] Liu, A., and Ziebart, B. D. (2014), “Robust Classification Under Sample Selection Bias.” in *NIPS*, pp. 37–45.
- [53] Lochner, M., McEwen, J. D., Peiris, H. V., Lahav, O., and Winter, M. K. (2016), “Photometric supernova classification with machine learning,” *The Astrophysical Journal Supplement Series*, 225, 31.
- [54] Loog, M. (2012), “Nearest neighbor-based importance weighting,” in *2012 IEEE International Workshop on Machine Learning for Signal Processing*, IEEE, pp. 1–6.
- [55] Lunceford, J. K., and Davidian, M. (2004), “Stratification and weighting via the propensity score in estimation of causal treatment effects: a comparative study,” *Statistics in medicine*, 23, 2937–2960.
- [56] Magliacane, S., van Ommen, T., Claassen, T., Bongers, S., Versteeg, P., and Mooij, J. M. (2018), “Domain adaptation by using causal inference to predict invariant conditional distributions,” in *Advances in Neural Information Processing Systems*, pp. 10846–10856.
- [57] Möller, A., and de Boissière, T. (2020), “SuperNNova: an open-source framework for Bayesian, neural network-based supernova classification,” *Monthly Notices of the Royal Astronomical Society*, 491, 4277–4293.
- [58] Moreno-Torres, J. G., Raeder, T., Alaiz-Rodríguez, R., Chawla, N. V., and Herrera, F. (2012), “A unifying view on dataset shift in classification,” *Pattern Recognition*, 45, 521–530.
- [59] Pan, S. J., Tsang, I. W., Kwok, J. T., and Yang, Q. (2010), “Domain adaptation via transfer component analysis,” *IEEE Transactions on Neural Networks*, 22, 199–210.
- [60] Pan, S. J.— (2009), “A survey on transfer learning,” *IEEE Transactions on knowledge and data engineering*, 22, 1345–1359.
- [61] Pasquet, J., Pasquet, J., Chaumont, M., and Fouchez, D. (2019), “Pelican: deep architecture for the light curve analysis,” *Astronomy & Astrophysics*, 627, A21.
- [62] Patel, V. M., Gopalan, R., Li, R., and Chellappa, R. (2015), “Visual domain adaptation: A survey of recent advances,” *IEEE signal processing magazine*, 32, 53–69.
- [63] Perlmutter, S., Aldering, G., Goldhaber, G., Knop, R., Nugent, P., Castro, P., Deustua, S., Fabbro, S., Goobar, A., Groom, D. et al. (1999), “Measurements of Ω and Λ from 42 high-redshift supernovae,” *The Astrophysical Journal*, 517, 565.
- [64] Quionero-Candela, J., Sugiyama, M., Schwaighofer, A., and Lawrence, N. D. (2009), *Dataset shift in machine learning*, The MIT Press.
- [65] Reddi, S., Poczos, B., and Smola, A. (2015), “Doubly robust covariate shift correction,” in *Proceedings of the AAAI Conference on Artificial Intelligence*, vol. 29.
- [66] Revsbech, E. A., Trotta, R., and van Dyk, D. A. (2018), “STACCATO: a novel solution to supernova photometric classification with biased training sets,” *Monthly Notices of the Royal Astronomical Society*, 473, 3969–3986.
- [67] Richards, J. W., Homrighausen, D., Freeman, P. E., Schafer, C. M., and Poznanski, D. (2012), “Semi-supervised learning for photometric supernova classification,” *Monthly Notices of the Royal Astronomical Society*, 419, 1121–1135.
- [68] Riess, A. G., Filippenko, A. V., Challis, P., Clocchiatti, A., Diercks, A., Garnavich, P. M., Gilliland, R. L., Hogan, C. J., Jha, S., Kirshner, R. P. et al. (1998), “Observational evidence from supernovae for an accelerating universe and a cosmological constant,” *The Astronomical Journal*, 116, 1009.
- [69] Rivera, W. A., Goel, A., and Kincaid, J. P. (2014), “OUPS: a combined approach using SMOTE and Propensity Score Matching,” in *2014 13th International Conference on Machine Learning and Applications*, IEEE, pp. 424–427.

- [70] Rojas-Carulla, M., Schölkopf, B., Turner, R., and Peters, J. (2018), “Invariant models for causal transfer learning,” *The Journal of Machine Learning Research*, 19, 1309–1342.
- [71] Rosenbaum, P. R. (1987), “Model-based direct adjustment,” *Journal of the American Statistical Association*, 82, 387–394.
- [72] Rosenbaum, P. R., and Rubin, D. B. (1983), “The central role of the propensity score in observational studies for causal effects,” *Biometrika*, 70, 41–55.
- [73] Rosenbaum, P. R.— (1984), “Reducing bias in observational studies using subclassification on the propensity score,” *Journal of the American statistical Association*, 79, 516–524.
- [74] Schnabel, T., Swaminathan, A., Singh, A., Chandak, N., and Joachims, T. (2016), “Recommendations as treatments: Debiasing learning and evaluation,” in *international conference on machine learning*, PMLR, pp. 1670–1679.
- [75] Sheldon, E. S., Cunha, C. E., Mandelbaum, R., Brinkmann, J., and Weaver, B. A. (2012), “Photometric redshift probability distributions for galaxies in the SDSS DR8,” *The Astrophysical Journal Supplement Series*, 201, 32.
- [76] Shimodaira, H. (2000), “Improving predictive inference under covariate shift by weighting the log-likelihood function,” *Journal of statistical planning and inference*, 90, 227–244.
- [77] Skeem, J. L., and Lowenkamp, C. T. (2016), “Risk, Race, & Recidivism: Predictive Bias and Disparate Impact.(2016),” *Criminology*, 54, 680.
- [78] Stojanov, P., Gong, M., Carbonell, J., and Zhang, K. (2019), “Low-dimensional density ratio estimation for covariate shift correction,” in *The 22nd International Conference on Artificial Intelligence and Statistics*, PMLR, pp. 3449–3458.
- [79] Stonnington, C. M., Tan, G., Klöppel, S., Chu, C., Draganski, B., Jack Jr, C. R., Chen, K., Ashburner, J., and Frackowiak, R. S. (2008), “Interpreting scan data acquired from multiple scanners: a study with Alzheimer’s disease,” *Neuroimage*, 39, 1180–1185.
- [80] Sugiyama, M., Krauledat, M., and Müller, K.-R. (2007), “Covariate shift adaptation by importance weighted cross validation,” *Journal of Machine Learning Research*, 8, 985–1005.
- [81] Sugiyama, M., and Müller, K.-R. (2005), “Input-dependent estimation of generalization error under covariate shift,” *Statistics & Risk Modeling*, 23, 249–279.
- [82] Sugiyama, M., Nakajima, S., Kashima, H., Buenau, P. V., and Kawanabe, M. (2008), “Direct importance estimation with model selection and its application to covariate shift adaptation,” in *Advances in neural information processing systems*, pp. 1433–1440.
- [83] Sugiyama, M., Yamada, M., Von Buenau, P., Suzuki, T., Kanamori, T.— (2011), “Direct density-ratio estimation with dimensionality reduction via least-squares hetero-distributional subspace search,” *Neural Networks*, 24, 183–198.
- [84] Suresh, H., and Gutttag, J. V. (2019), “A framework for understanding unintended consequences of machine learning,” *arXiv preprint arXiv:1901.10002*.
- [85] Tai, L., Paolo, G., and Liu, M. (2017), “Virtual-to-real deep reinforcement learning: Continuous control of mobile robots for mapless navigation,” in *2017 IEEE/RSJ International Conference on Intelligent Robots and Systems (IROS)*, IEEE, pp. 31–36.
- [86] Tsuboi, Y., Kashima, H., Hido, S., Bickel, S., and Sugiyama, M. (2009), “Direct density ratio estimation for large-scale covariate shift adaptation,” *Journal of Information Processing*, 17, 138–155.
- [87] Umer, M., Frederickson, C., and Polikar, R. (2019), “Vulnerability of Covariate Shift Adaptation Against Malicious Poisoning Attacks,” in *2019 International Joint Conference on Neural Networks (IJCNN)*, IEEE, pp. 1–8.
- [88] Van Erven, T., and Harremos, P. (2014), “Rényi divergence and Kullback-Leibler divergence,” *IEEE Transactions on Information Theory*, 60, 3797–3820.

- [89] Van Opbroek, A., Ikram, M. A., Vernooij, M. W., and De Bruijne, M. (2014), “Transfer learning improves supervised image segmentation across imaging protocols,” *IEEE transactions on medical imaging*, 34, 1018–1030.
- [90] Vilalta, R., Gupta, K. D., and Macri, L. (2013), “A machine learning approach to Cepheid variable star classification using data alignment and maximum likelihood,” *Astronomy and Computing*, 2, 46–53.
- [91] Villar, V., Berger, E., Miller, G., Chornock, R., Rest, A., Jones, D., Drout, M., Foley, R., Kirshner, R., Lunnan, R. et al. (2019), “Supernova Photometric Classification Pipelines Trained on Spectroscopically Classified Supernovae from the Pan-STARRS1 Medium-Deep Survey,” *The Astrophysical Journal*, 884, 83.
- [92] Wen, J., Greiner, R., and Schuurmans, D. (2015), “Correcting covariate shift with the Frank-Wolfe algorithm,” in *Twenty-Fourth International Joint Conference on Artificial Intelligence*.
- [93] Wen, J., Yu, C.-N., and Greiner, R. (2014), “Robust learning under uncertain test distributions: Relating covariate shift to model misspecification,” in *International Conference on Machine Learning*, PMLR, pp. 631–639.
- [94] Yoon, J., Zhang, Y., Jordon, J., and van der Schaar, M. (2020), “VIME: Extending the Success of Self-and Semi-supervised Learning to Tabular Domain,” *Advances in Neural Information Processing Systems*, 33.
- [95] Yu, Y., and Szepesvári, C. (2012), “Analysis of kernel mean matching under covariate shift,” *arXiv preprint arXiv:1206.4650*.
- [96] Zadrozny, B. (2004), “Learning and evaluating classifiers under sample selection bias,” in *Proceedings of the twenty-first international conference on Machine learning*, ACM, p. 114.

6 Supplement – Additional information for Section 3 (Methodology – Covariate Shift adjustment through Stratified Learning)

Verification of Proposition 3: For Proposition 3, we start from [Theorem 1] in [72], which proves that the propensity score $e(x)$, with $0 < e(x) < 1$, is a balancing score, which for our case means

$$x \perp\!\!\!\perp s | e(x), \quad (12)$$

or equivalently $p_S(x|e(x)) = p_T(x|e(x))$. That is, conditional on the propensity score, the covariates in the source and target data have the same distribution. It follows that

$$\begin{aligned} p_S(x, y|e(x)) &:= p(x, y|e(x), s = 1) \\ &= p(y|x, e(x), s = 1)p(x|e(x), s = 1) \end{aligned} \quad (13)$$

$$= p(y|x, e(x), s = 0)p(x|e(x), s = 1) \quad (14)$$

$$= p(y|x, e(x), s = 0)p(x|e(x), s = 0) \quad (15)$$

$$= p(x, y|e(x), s = 0)$$

$$=: p_T(x, y|e(x)).$$

Step (14) follows from the covariate shift assumption that $p(y|x, s = 1) = p(y|x, s = 0)$, with $e(x)$ as a function of x not changing the conditional distributions. Step (15) follows from the balancing property of the propensity score (12). Thus, conditional on the propensity score, the source and target data have the same joint distribution. Equation (6) follows directly.

In the propensity score literature, a form of (12) is often used to verify the propensity score model and/or the suitability of the choice of covariates, x , e.g. by checking that x has the same within-strata distribution in the treatment and control groups. Measures such as standardized mean differences, the Kolmogorov-Smirnov test statistics, or comparison of higher order moments and interaction terms are used to assess the covariate balance [S1;S2] [4; 73]. As detailed in Remark 1, we can exploit additional structure in the covariate shift setting to justify a corollary model diagnostic.

Remark 1. *In the propensity score framework of causal inference [72] we have potential outcomes Y_0 and Y_1 , where Y_1 is only observed in the treated (source) group and Y_0 is only observed in the control (target) group. In the covariate shift framework, the potential outcomes are identical ($Y_0 \equiv Y_1$). That is, there is no “treatment effect” from being assigned to the source or target set, though only the source data is observed ($Y_1 \equiv Y$). Now, given the propensity score $e(x)$, with $0 < e(x) < 1$, and the covariate shift condition $p(y|x, s = 1) = p(y|x, s = 0)$, source data assignment is ‘strongly ignorable’ (using the terminology of [72]). It follows through Theorem 4 in [72] that, conditional on the propensity score, source and target outcome are the same in expectation.*

In cases where labels are observed for (part of) the target group we can use Remark 1 as a model diagnostic. Although in practice the labels are unobserved in the target group, they are observed in our real-world scientific/experimental settings described in Sections 4.3 and 4.4. In Sections 10, 11, 12 and 13, we use Remark 1 to demonstrate a reduction of within-strata covariate shift (i.e., by conditioning on the propensity score). (A future project is to explore the possibility of similarly using predicted labels instead of actual labels in a model diagnostic.)

7 Supplement – Additional specifications for Section 4.1 (Comparison Models)

Here we detail our implementation of the several methods listed in Section 4.1 that we compare with *StratLearn* in our numerical studies.

Importance weighting estimators: Following [42] and [1], by Bayes Theorem,

$$w(x) = \frac{p_T(x)}{p_S(x)} = \frac{p(s = 1)}{p(s = 0)} \frac{p(s = 0|x)}{p(s = 1|x)} \approx \frac{n_S}{n_T} \left(\frac{1}{p(s = 1|x)} - 1 \right). \quad (16)$$

The importance weighting based estimators, KLIEP, uLSIF and NN, (described in Section 4.1) directly estimate $w(x)$. IPS obtains an estimate of $w(x)$ by plugging in the estimated propensity

score into the right hand side of (16). The estimated weights in (16) can then be used for weighted empirical risk minimization (following Proposition 1); e.g., through (10) in Section 4.4, through WLS in Section 4.2, and through IWCV in Section 4.3.

To implement importance sampling, such as in Section 4.3, we follow Proposition 2 and directly use the inverse of the estimated propensity scores. Moreover, rearranging the terms in the formulation of $w(x)$ in the right hand side of (16) yields

$$p(s=0)w(x) + p(s=1) = \frac{p(s=1)}{p(s=1|x)}. \quad (17)$$

Then, substituting into (3),

$$\hat{\mathcal{D}}(x, y, s) := \frac{P(s=1)}{P(s=1|x)} \mathcal{D}(x, y, s) \quad (18)$$

$$= (w(x)p(s=0) + p(s=1)) \mathcal{D}(x, y, s). \quad (19)$$

Thus, following Proposition 2, IPS can be used for importance sampling via (18), and the direct weight estimators KLIEP, uLSIF and NN can be used for importance sampling via (19).

8 Supplement – Data and software

We provide software, data and instructions to reproduce the numerical results presented in this paper on request. The data used for photometric redshift regression, as presented in Section 4.4 was used by permission of the original authors of [75]. The data used from the UCI repository [25] is publicly available and can be accessed here (UCI Wine quality data (link), Parkinsons Telemonitoring Data (link)).

The *StratLearn* software that we provide is written in R [S6]. For computation of the experiments, a 32 CPU Core cluster was available to speed up the simulations. However, computation time/resources was not a significant issue for the numerical results in this paper. As a benchmark, using a MacBook Pro with a 2.3 GHz 8-Core i9 processor, one scenario (e.g., medium covariate shift, high-dimensional covariate set) for conditional density estimation on SDSS data, took less than 8 hours to run. All other experiments are less time-consuming. The supernova classification (Section 4.3) on preprocessed SPCC data took less than 2 hours, on the same MacBook Pro.

9 Supplement – Additional results for Section 4.2 (Regression – Univariate example)

Section 4.2 describes a numerical experiment using a well known univariate example from [76]. To ensure that there is sufficient data in the last stratum when implementing this example, we add the source data from stratum 4 to that of stratum 5 in cases where replicate data had fewer than 10 source samples in stratum 5. Here we replicate these results using a minimum threshold of 5 source samples (instead of 10); Figure 4 presents *StratLearn* results and shows very similar performance to the results in Figure 1 (which used a threshold of 10 source samples), demonstrating robustness with respect to the choice of this threshold.

Table 1 presents the mean and standard error (se) of the $m = 1000$ target MSE's presented in Figures 1 and 4, illustrating the superior performance of *StratLearn* in covariate shift examples (ii) and (iii) of Section 4.2, and further demonstrating its robustness with respect to the choice of the combination rule.

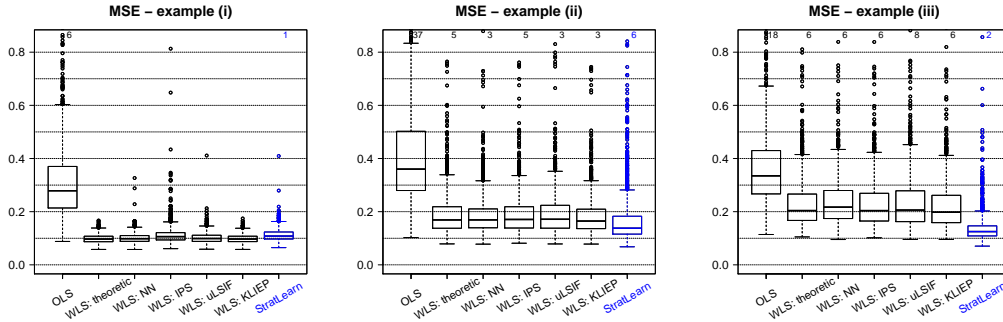


Figure 4: Boxplot of the target MSE, obtained by fitting the models on the same $m = 1000$ Monte Carlo simulations as presented in Figure 1 (examples (i) to (iii) from left to right). To ensure that there is enough source data in the last stratum, the source data from stratum 4 was added to fit the model for stratum 5 in cases where replicate data had fewer than 5 source samples in stratum 5 (instead of a minimum of 10 samples as in Figure 1). The *StratLearn* results are very similar compared to Figure 1, demonstrating robustness with respect to this combination rule.

Table 1: Mean and standard error (se) of the $m = 1000$ target MSE's presented in Figures 1 and 4 (examples (i) to (iii) from left to right). *StratLearn* (min = 10) refers to values presented in Figure 1, where source data from stratum 4 was added to fit the model for stratum 5 in cases where replicate data had fewer than 10 source samples in stratum 5, to ensure that there is enough source data in the last stratum. *StratLearn* (min = 5) refers to values presented in Figure 4, using a minimum of 5 samples in source stratum 5 as a combination rule. Best model performances are highlighted in bold.

Method \ MSE	Example (i):		Example (ii):		Example (iii):	
	Mean	(se)	Mean	(se)	Mean	(se)
OLS	0.312	(0.148)	0.415	(0.208)	0.370	(0.173)
WLS: theoretical	0.098	(0.016)	0.196	(0.109)	0.239	(0.131)
WLS: NN	0.101	(0.020)	0.189	(0.088)	0.244	(0.123)
WLS: IPS	0.115	(0.045)	0.196	(0.108)	0.236	(0.130)
WLS: uLSIF	0.102	(0.022)	0.197	(0.101)	0.243	(0.140)
WLS: KLIEP	0.098	(0.016)	0.188	(0.095)	0.229	(0.126)
StratLearn (min = 10)	0.108	(0.023)	0.181	(0.108)	0.140	(0.076)
StratLearn (min = 5)	0.113	(0.040)	0.178	(0.143)	0.141	(0.077)

10 Supplement – Additional results for Section 4.3 (Classification – Supernova photometric classification challenge)

Section 4.3 describes the classification of supernovae (SNe) into type 1a (SNIa) and non SNIa based on photometric light curve data, given a strongly biased source data set. Table 2 presents the composition of the five *StratLearn* strata obtained by conditioning the updated SPCC data on the estimated propensity scores, as described in Section 4.3. The SNIa proportions align well in the first two strata, indicating a reduction in covariate shift, as expected from Remark 1. The source sample sizes in strata 3-5 are quite small, and meaningful comparison of the SNIa proportions in these strata is not possible.

Table 2: Composition of the five *StratLearn* strata on the updated SPCC data (as referred to in Section 4.3). The number of SNe, as well as the number and proportion of SNIa are presented in each source and target stratum.

Stratum	Set	Number of SNe	Number of SNIa	Prop. of SNIa
1	Source	958	518	0.54
	Target	3306	1790	0.54
2	Source	120	28	0.23
	Target	4144	927	0.22
3	Source	13	4	0.31
	Target	4250	540	0.13
4	Source	7	4	0.57
	Target	4257	610	0.14
5	Source	4	4	1
	Target	4259	662	0.16

Random forest implementation and hyperparameter selection: We use the “ranger” random forest implementation in *caret* [S4] for SNe classification in this paper. Repeated 10-fold cross-validation (with five repetitions) is implemented with a large hyperparameter grid, containing four different numbers of covariates to possibly split at in each node (3,5,8,10); five values for minimum node size (3,5,7,10,20); and two different splitting rules (“gini” and “extratrees”). The best hyperparameter setting is selected by optimization of the cross-validated AUC. Using *StratLearn* cross-validation for hyperparameter selection (optimizing the AUC) is done on each source group separately (with groups defined in Section 4.3).

Comparison of importance weighting methods: In addition to importance sampling (as presented in Figure 2), we investigate two further importance weighting approaches to obtain a comprehensive performance comparison of importance weighting and *StratLearn*. More precisely, we implement IWCV, and a combination of IWCV and importance sampling. Table 3 presents the resulting target AUC for all implemented weighting methods. In summary, none of the importance weighting methods are competitive with *StratLearn*, which obtained a target AUC of 0.958. In fact, using IWCV alone leads to a decrease in performance for NN (0.897) and IPS (0.897) relative to the “Biased” fit (0.902). In order to reweight the loss of each object separately when implementing IWCV, we optimize with respect to the log-loss instead of AUC. We do not expect this to be responsible for the decreased target performance. For example, using log-loss as the hyperparameter selection criterion for *StratLearn* in each source group (instead of AUC) leads to the same target AUC of 0.958. Importance sampling is the only weighting method for which we present the associated ROC curve in Figure 2, because it has the highest average AUC.

11 Supplement – StratLearn applied to original SPCC data [45]

Data: We investigate the performance of *StratLearn* on data from the original “Supernova photometric classification challenge” (SPCC) [45] – an earlier version of the SPCC data described in Section 4.3, mainly for comparison with previous literature that use the original SPCC data. The earlier version of the SPCC data features a total of 17,330 simulated SNe of type Ia (SNIa), Ib, Ic and

Table 3: AUC results on the updated SPCC (photometric) target data [44], using various importance weighting approaches to adjust for covariate shift.

	IWCV	importance sampling	IWCV + importance sampling
uLSIF	0.906	0.902	0.906
NN	0.897	0.923	0.914
IPS	0.897	0.921	0.924

Table 4: Composition of the five strata on the original SPCC data [45]. The number of SNe, as well as the number and proportion of SNIa are presented in each source and target stratum.

Stratum	Set	Number of SNe	Number of SNIa	Prop. of SNIa
1	Source	996	794	0.80
	Target	2470	1759	0.71
2	Source	210	56	0.27
	Target	3256	1010	0.31
3	Source	9	0	0
	Target	3457	385	0.11
4	Source	2	1	0.50
	Target	3464	258	0.07
5	Source	0	0	NA
	Target	3466	180	0.05

II. The data set is divided into a source (training) set D_S of 1,217 spectroscopically confirmed SNe with known types and 16,113 SNe with unknown types and photometric information alone (target set) D_T . The simulation used to generate the original SPCC data suffered from a bug that made classification easier, thus leading to the updated SPCC data used in Section 4.3. As in Section 4.3, we applied GP fitting and diffusion maps [66; 67] to obtain a set of 102 predictive covariates; 100 covariates from the diffusion map, plus redshift (defined in Section 4.4) and a measure of the objects’ brightness [66].

Results: Table 4 presents the composition of the five strata obtained by conditioning on the estimated propensity scores, exhibiting a similar pattern as the strata composition on the updated SPCC data (Table 2), though with a higher proportion of SNIa in the first stratum and even less source data in strata 3 – 5. We thus follow the same strategy as described in Section 4.3. After stratification, a random forest classifier is trained and optimized on source strata D_{S_1} and D_{S_2} separately to classify SNe in target strata D_{T_1} and D_{T_2} , respectively. Source strata D_{S_j} for $j \in \{3, 4, 5\}$ are merged with D_{S_2} to train the random forest to predict D_{T_j} for $j \in \{3, 4, 5\}$. Repeated 10-fold cross validation (with the hyperparameter grid described in Section 10) is performed to minimize the empirical risk of (9) within each group.

With *StratLearn* we obtain an AUC of 0.977 on the target data of the original SPCC data (blue ROC curve in Figure 5), very near the optimal ‘gold standard’ benchmark, which is 0.982 on this data set (obtained on a randomly resampled source data set, which would not exhibit covariate shift and would not be available in practice). The AUC obtained with *StratLearn* is also larger than the previous best published AUC for this data, obtained with STACCATO via a data augmentation strategy, AUC = 0.961 [66]. Note that the predictive target performance on the original SPCC data [45] is generally higher than on the updated version [44], because the aforementioned bug made classification of the original data easier.

Most of the importance weighting methods (Table 5) lead to slight improvements over the (non-adjusted) “biased” model fit. The best performing weighting approaches (using estimated NN or IPS weights for importance sampling) obtain target AUC of 0.942, substantially lower than *StratLearn* (AUC: 0.977). Importance sampling is the only weighting method for which we present the associated ROC curve in Figure 5, because it has the highest average AUC.

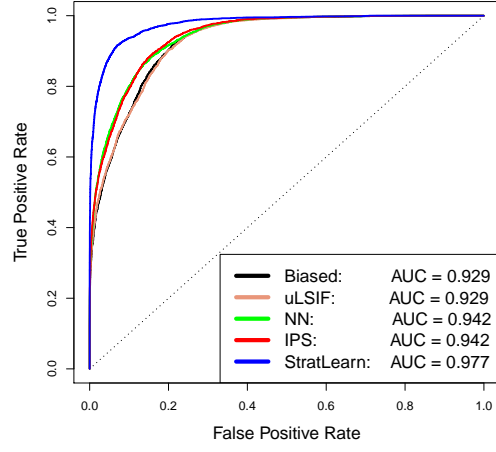


Figure 5: Comparison of ROC curves for SNIa classification using the original SPCC data.

Table 5: AUC results on the original SPCC (photometric) target data [45], using various importance weighting approaches to adjust for covariate shift.

	IWCV	importance sampling	IWCV + importance sampling
uLSIF	0.934	0.929	0.936
NN	0.934	0.942	0.931
IPS	0.934	0.942	0.931

12 Supplement – Additional numerical evidence on data from the UCI repository [25]

In this section, we are particularly interested in demonstrating the performance of *StratLearn* under violation of the covariate shift assumption. We apply *StratLearn* on two datasets from the publicly available UCI repository [25]: the "wine quality data" [S3] and the "Parkinson Telemonitoring data" [S5]. These datasets have previously been used to explore regression problems in the presence of covariate shift [17]. Links to the used data sets can be found in Section 8.

12.1 Data description

Wine quality data: The data set contains 6497 samples of which 4898 are of type "white wine", used as source data D_S , and 1599 samples are of type "red wine", used as the target data D_T . The output is a wine "quality score" (between 0 and 10), which we aim to predict for the target data (red wine), given the scores of the source data (white wine). There are 11 physicochemical, predictive covariates. We refer to [S3] for detailed information.

Parkinson data: The data comprises 5875 instances and 26 attributes. Similar to [17], we take 17 of the attributes to be predictive covariates, with the aim of predicting the UPDRS Parkinson's disease symptom score (output). The source data D_S contains all instances with age below 60, leading to a source subset of size $|D_S| = 1877$. Instances with age above (inclusively) 60 and below 70 are used as target samples D_T , with $|D_T| = 2127$. As in [17], instances with age above 70 are not considered. We refer to [S5] for further information on the data.

12.2 Implementation and results on UCI data

Following [17], our objective is to predict the wine "quality score" and the Parkinson's "UPDRS" score using linear regression models, specifically ordinary least squares (OLS). We assume that the source and target splitting covariates (wine type and age) are not observed for model fitting. Note that, because these are confounding covariates, this violates the covariate shift assumption. All other available covariates are used to estimate the propensity scores and the importance weights, and as predictor variables for the outcome models. To improve covariate balance on the wine quality data, we used gradient boosting machines to estimate the propensity scores, commonly used in the propensity score causal inference literature [S7;S8]. Covariate balance was assessed as described in Section 6.

Table 6 presents the composition of the *StratLearn* strata for the Wine and Parkinson data, both conditioned on the estimated propensity scores. For the wine data set, all target samples are in strata 4 and 5, and only stratum 4 contains both source and target samples. Following our *StratLearn* strategy, we fit OLS on D_{S_4} to predict D_{T_4} and D_{T_5} . In the Parkinson data set there is enough source data in each strata to fit OLS separately on each source stratum D_{S_j} to predict the data in the respective target stratum D_{T_j} , $j \in \{1, \dots, 5\}$.

Table 7 presents the MSE of the target predictions, comparing *StratLearn* with (non-adjusted) OLS ("Biased") and WLS, using the methods described in Section 4.1 to estimate the weights. Applying *StratLearn* results in a target MSE of 0.715 for the Wine data and 114.97 for the Parkinson data, both improving upon the "Biased" OLS fit which yields a target MSE of 1.024 (Wine) and 130.88 (Parkinson). *StratLearn* further provides better results than WLS:uLSIF, WLS:KLIEP and WLS:NN on both data sets, only WLS:IPS leads to slightly better results than *StratLearn*.

We also compare *StratLearn* with the method that [17] develops and illustrates on these datasets. Specifically, [17] proposes a "robust bias-aware regression" based on the Kullback-Leibler divergence. This proposal is tailored specifically to regression and to loss functions that account for uncertainty in the prediction (e.g., empirical logloss), whereas *StratLearn* is entirely general, but can be successfully applied to this task. Following [17], we compute the target empirical logloss as a performance measure. On the Wine data, *StratLearn* yields an empirical logloss of 1.271, which exactly matches the reported performance of the method proposed in [17]. On the Parkinson data we could not replicate the exact data split as reported in [17], a meaningful comparison of empirical logloss to the values reported by [17] is thus not possible.

In summary, in these illustrative regression examples *StratLearn* demonstrates certain robustness against violation of the covariate shift assumption, improving upon the (non-adjusted) “Biased” fit and performing comparably with the best importance weighting approach.

Table 6: Composition of the five *StratLearn* strata for the UCI wine and UCI parkinson data. The number of samples/subjects in source and target stratum, as well as the mean outcome (“quality score” and “UPDRS score”) are presented.

Stratum	Set	UCI Wine data	UCI Parkinson data
		# samples (Mean “quality”)	# subjects (Mean “UPDRS”)
1	Source	1299 (5.98)	627 (22.00)
	Target	0 (0.00)	174 (29.15)
2	Source	1300 (5.92)	486 (26.36)
	Target	0 (0.00)	315 (25.21)
3	Source	1300 (5.93)	314 (25.53)
	Target	0 (0.00)	487 (24.86)
4	Source	999 (5.63)	269 (27.38)
	Target	301 (5.49)	532 (28.15)
5	Source	0 (0.00)	181 (27.06)
	Target	1298 (5.67)	619 (30.00)
All	Source	4898 (5.88)	1877 (24.98)
	Target	1599 (5.64)	2127 (27.58)

Table 7: MSE of target predictions on UCI Wine and Parkinson data, based on ordinary least squares regression (OLS), various importance weighted least squares regression methods (WLS), and our proposed *StratLearn* method.

Method \ Data	UCI wine data	UCI Parkinson data
OLS (Biased)	1.024	130.88
WLS:uLSIF	2.363	120.81
WLS:KLIEP	3.968	116.72
WLS:NN	2.377	117.47
WLS:IPS	0.660	112.80
StratLearn	0.715	114.97

13 Supplement – Additional results for Section 4.4 (Full conditional density estimation – Photometric redshift regression)

Additional covariate shift setups: In the context of the photometric redshift regression example in Section 4.4, we present additional numerical results that demonstrate the robustness of *StratLearn* to varying degrees of covariate shift. Specifically, we reproduce the results of Section 4.4, but under two additional covariate shift scenarios. We use the same data setup as in Section 4.4, but change the rejection sampling used to simulate an unrepresentative target D_T from D_S , to

- Weak covariate shift:

$$p(s=0|x) = f_{B(9,4)}(x_{(r)}) / \max_{x_{(r)}} f_{B(9,4)}(x_{(r)}) \quad (20)$$

- Strong covariate shift:

$$p(s=0|x) = f_{B(18,4)}(x_{(r)}) / \max_{x_{(r)}} f_{B(18,4)}(x_{(r)}), \quad (21)$$

where $x_{(r)}$ is the r -band magnitude and $f_{B(9,4)}$ and $f_{B(18,4)}$ are beta densities with parameters (9,4) and (18,4), respectively. Except for the adjusted degree of covariate shift, simulations are performed as described in Section 4.4.

The target risk $\hat{R}_T(\hat{f})$, as described in Section 4.4 and shown in Figure 3 and 6, is computed as

$$\hat{R}_T(\hat{f}) = \frac{1}{n_T} \sum_{k=1}^{n_T} \int \hat{f}^2(z|x_T^{(k)}) dz - 2 \frac{1}{n_T} \sum_{k=1}^{n_T} \hat{f}(z_T^{(k)}|x_T^{(k)}), \quad (22)$$

where z_T is the true target redshift, which is known but used for evaluation purposes only.

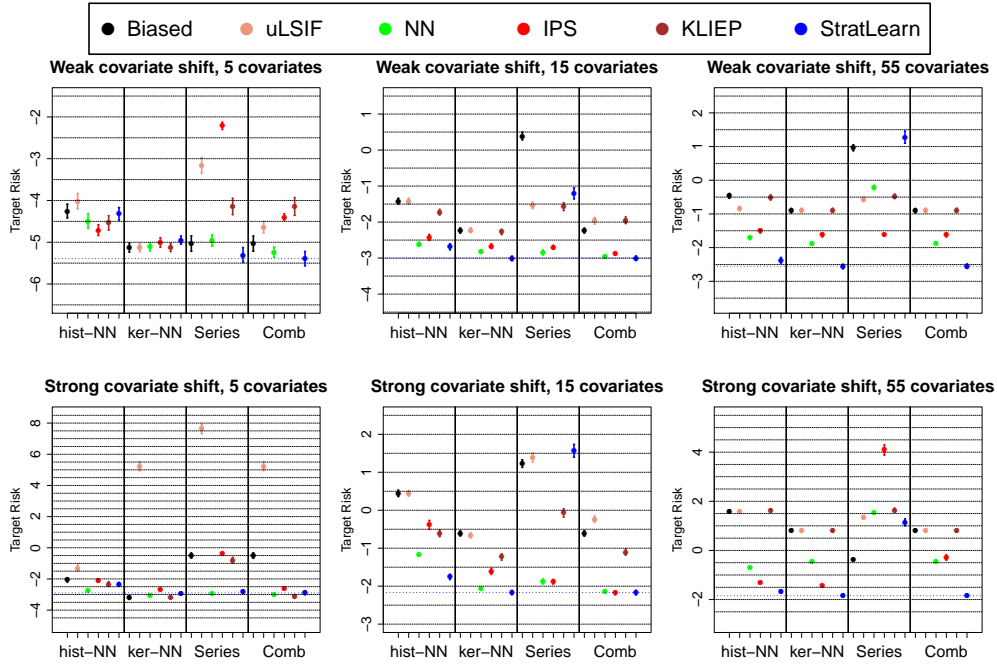


Figure 6: Target risk (\hat{R}_T) of photometric redshift estimation models, using different sets of predictors. Bars give the mean ± 2 bootstrap standard errors (from 400 bootstrap samples). Top row: Weak covariate shift (following (20)); Bottom row: Strong covariate shift (following (21)).

Table 8: Composition of the five *StratLearn* strata for the medium covariate shift scenario (as described in Section 4.4) on SDSS data, using estimated propensity scores with different sets of predictors. The number of galaxies in source and target stratum, as well as the mean outcome (redshift z) are presented.

Stratum	Set	5 covariates	15 covariates	55 covariates
		#galaxies (Mean z)	#galaxies (Mean z)	#galaxies (Mean z)
1	Source	1631 (0.06)	1583 (0.06)	1620 (0.06)
	Target	7 (0.05)	9 (0.05)	7 (0.05)
2	Source	1500 (0.09)	1515 (0.09)	1546 (0.09)
	Target	112 (0.08)	113 (0.09)	98 (0.08)
3	Source	618 (0.20)	641 (0.20)	594 (0.21)
	Target	1481 (0.23)	1499 (0.23)	1480 (0.23)
4	Source	116 (0.30)	114 (0.28)	108 (0.28)
	Target	2196 (0.27)	2215 (0.27)	2258 (0.27)
5	Source	135 (0.33)	147 (0.32)	132 (0.33)
	Target	2204 (0.33)	2164 (0.34)	2157 (0.34)
All	Source	4000 (0.11)	4000 (0.11)	4000 (0.11)
	Target	6000 (0.28)	6000 (0.28)	6000 (0.28)

Table 9: Composition of the five *StratLearn* strata for the weak covariate shift (20) and strong covariate shift (21) scenarios on SDSS data, using a set of five predictors for propensity score estimation. The number of galaxies in source and target stratum, as well as the mean outcome (redshift z) are presented.

Stratum	Set	weak covariate shift, 5 covariates	strong covariate shift, 5 covariates
		#galaxies (Mean z)	#galaxies (Mean z)
1	Source	1468 (0.06)	1603 (0.05)
	Target	145 (0.06)	0 (0)
2	Source	1220 (0.09)	1579 (0.07)
	Target	602 (0.08)	4 (0.07)
3	Source	740 (0.14)	637 (0.17)
	Target	1275 (0.15)	1494 (0.20)
4	Source	301 (0.26)	73 (0.25)
	Target	1958 (0.26)	2297 (0.23)
5	Source	271 (0.33)	108 (0.29)
	Target	2020 (0.31)	2205 (0.26)
All	Source	4000 (0.12)	4000 (0.09)
	Target	6000 (0.23)	6000 (0.24)

Summary – conditional density estimation: Figure 6 compares the resulting target risk $\hat{R}_T(\hat{f})$ across models and covariate sets, for the weak covariate shift (top row) and the strong covariate shift scenario (bottom row). These results, combined with those from the medium covariate shift scenario in Figure 3, reinforce the advantage of using *StratLearn*, especially for higher dimensional covariate sets. In Figures 3 and 6, *StratLearn_{Series}* performs well in the setup with the fewest covariates (left column). In the weak covariate shift scenario, this leads to an additional boost in performance of *StratLearn_{Comb}* (which combines *StratLearn_{ker-NN}* and *StratLearn_{Series}*, following (11)). In the setups with higher dimensional covariates, the Series methods (using either *StratLearn* or the weighting methods) exhibit relatively poor performance overall. In these cases, the *StratLearn_{Comb}* predictions rely solely on *StratLearn_{ker-NN}*, which again demonstrates the successful empirical risk minimization of (9), inasmuch as *StratLearn_{Comb}* automatically selects the better *target* model (i.e., *StratLearn_{ker-NN}*) in each stratum, based on the respective empirical *source* risk estimates in each stratum. Overall, IPS and NN weighting are most competitive with *StratLearn*, in addition to KLIEP in the low dimensional, strong covariate shift setup. Note that the performances of *IPS_{Comb}*, *KLIEP_{Comb}* and *uLSIF_{Comb}* are degraded in some cases (e.g., Figure 6, upper left panel) with inclusion of the poorly performing *Series* predictions, illustrating that the weighted empirical *source* risk minimization ((10), as a form of (1)) does not lead to *target* risk minimization in these situations. With increasing number of covariates, none of the weighted models yield results that are competitive with *StratLearn*.

Table 13 presents the composition of the five *StratLearn* strata for medium covariate shift scenario (described in Section 4.4) for each of the three sets of covariates. Each source stratum contains a sufficient sample size to fit the conditional density estimators for prediction on the respective target stratum. The overall redshift averages in the source (0.11) and target data (0.28) are very unequal, a consequence of the covariate shift. Within strata, the redshift averages are well aligned between source and target, indicating improved balance after stratification. Notably, the composition of the strata in the high-dimensional covariate setup is similar to the that of the lower-dimensional setups, with well-balanced strata. This is an indication of the robustness of *StratLearns* with respect to high dimensional (noisy) sets of covariates. Table 9 compares the five *StratLearn* strata for the weak and strong covariate shift scenarios, again with well-aligned average redshift within each stratum. Note that for the strong covariate shift scenario there are almost no galaxies in the first two target strata. Thus, effectively only data in source stratum 3 to 5 are used for target prediction in the respective strata. These examples illustrate the advantage of using only a small subset of the source data when formulating predictions for individuals in the target, where the subset is chosen for its similarity to the target data in question. This is a markedly different strategy to the widespread practice of including all possible available data when fitting machine learning models.

Supplement – References

- [S1] Austin, P. C. (2011), “An introduction to propensity score methods for reducing the effects of confounding in observational studies,” *Multivariate behavioral research*, 46, 399–424.
- [S2] Austin, P. C., Grootendorst, P., and Anderson, G. M. (2007), “A comparison of the ability of different propensity score models to balance measured variables between treated and untreated subjects: a Monte Carlo study,” *Statistics in medicine*, 26, 734–753.
- [S3] Cortez, P., Cerdeira, A., Almeida, F., Matos, T., and Reis, J. (2009), “Modeling wine preferences by data mining from physicochemical properties,” *Decision support systems*, 47, 547–553.
- [S4] Kuhn, M. (2008), “Building Predictive Models in R Using the caret Package,” *Journal of Statistical Software*, Articles, 28, 1–26.
- [S5] Little, M., McSharry, P., Hunter, E., Spielman, J., and Ramig, L. (2008), “Suitability of dysphonia measurements for telemonitoring of Parkinson’s disease,” *Nature Precedings*, 1–1.
- [S6] R Core Team (2019), *R: A Language and Environment for Statistical Computing*, R Foundation for Statistical Computing, Vienna, Austria.
- [S7] McCaffrey, D., Griffin, B. A., Almirall, D., Slaughter, M., Ramchand, R., and F Burgette, L. (2013), “A Tutorial on Propensity Score Estimation for Multiple Treatments Using Generalized Boosted Models,” 32.
- [S8] McCaffrey, D. F., Ridgeway, G., and Morral, A. R. (2004), “Propensity score estimation with boosted regression for evaluating causal effects in observational studies,” *Psychological methods*, 9, 403